

Pressuremeter tests within an active rock glacier in the Swiss Alps

L.U. Arenson

Institute for Geotechnical Engineering, Swiss Federal Institute of Technology, Zurich, Switzerland

P.G. Hawkins

Cambridge InSitu, Cambridge, United Kingdom

S.M. Springman

Institute for Geotechnical Engineering, Swiss Federal Institute of Technology, Zurich, Switzerland

ABSTRACT: In order to determine *in situ* creep and strength parameters of an active ice rich rock glacier in the Upper Engadin, Swiss Alps, pressuremeter tests were conducted using a 95 mm High Pressure Dilatometer. Seven tests were performed at different depths, immediately after the borehole had been drilled below the planned test level. A range of different loading steps were applied and these lasted up to 17 hours. In between the loading steps, unload-reload loops or strain holding (relaxation) tests were conducted. An attempt was made to reach failure at the end of each test. The results showed that the creep rate increased exponentially with the applied cavity pressure. The rate varied with depth and therefore with the ice content, which decreased from the highest test location to the lowest.

1 INTRODUCTION

Active rock glaciers are present in Switzerland at elevations above about 2500 metres above sea level, depending on local climatic and, in particular, solar radiation conditions. Since Alpine permafrost is highly sensitive to climate changes (Cheng & Dramis 1992, Haeberli et al. 1993), due to ground temperatures close to the melting point of ice, instabilities are likely to occur, triggering debris flows or rock avalanches (Haeberli et al. 1997).

Numerical modelling is potentially a useful method to aid judgement of the stability of a rock glacier and to be able to predict its future behaviour. However, constitutive models that are able to describe the temperature dependent soil behaviour are necessary for such modelling. The determination of such a model is very difficult, since rock glaciers are very diverse and extremely heterogeneous (Arenson et al. 2002). The internal structure varies with ice content (100% to 0%), grain sizes (some metres to silt size), unfrozen water content (as a function of the grain size and the temperature: Williams 1967) or air content (Arenson et al. 2003).

During recent years, various projects have been initiated in Alpine regions in order to improve the understanding of the thermal, hydraulic and mechanical processes relating to rock glaciers. Ground temperatures have been monitored throughout Europe (e.g. Harris et al. 2001) and geophysical investigations have been carried out from the surface and within boreholes to help to define the internal structure (Hauck et al. 2001, Musil et al. 2002). High

precision photogrammetry (Kääb & Vollmer 2000) is a valuable tool for measuring the spatial distribution of the surface deformation, and borehole deformation measurements reveal internal deformation profiles (e.g. Arenson & Springman 2000, Arenson et al. 2002).

However, all the methods and monitoring devices do not reveal information concerning the mechanical properties directly, such as shear strength or creep susceptibility of rock glacier material. Laboratory and *in situ* mechanical testing of frozen material may help, even though they represent only information for a particular point within a very heterogeneous body, and size effects have to be considered. (e.g. Fragaszy et al. 1990). These relate to the relative size of the soil volume influenced by the laboratory or *in situ* test and the representativity of this volume (e.g. as a function of the particle size distribution) with respect to the rock glacier as a whole.

The use of pressuremeters for the determination of *in situ* creep properties has already been recommended by Ladanyi & Johnston (1973) and has been used for many investigations within Arctic permafrost and ice (e.g. Ladanyi 1982, Ladanyi & Hun-eault 1987, Ladanyi and Melouki, 1992). This paper describes multi-stage creep pressuremeter tests using the Cambridge InSitu 95 mm High Pressure Dilatometer, which had been carried out for the first time in a pre-drilled borehole within an Alpine rock glacier. Due to the very heterogeneous structure, the borehole was only stable within ice-rich layers (i.e. vol. ice content > about 70%). The results of these tests are presented in this paper and compared with

triaxial creep tests, which have been carried out on samples from similar depths.

Creep effects have to be taken into account in the determination of stiffness and strength parameters. The shear moduli, which were derived from unload-reload loops during the pressuremeter tests, indicate tendentially a linear increase for mean radial stresses up to 1.5 GPa, where the influence of the mean stress appears to become insignificant. A lower yield stress between 2 and 3 MPa could be determined by allowing for the effect of creep using an exponential creep law based on the creep parameters calculated from the creep phases of the corresponding test. A limiting stress was only reached for two tests due to the large deformations necessary to cause failure, and this appears to depend on the applied volumetric strain rate. The limiting stress was found to be two to three times higher than the yield stress, and a higher value could be achieved at a lower radial strain rate.

2 SITE SPECIFICATION

Two new boreholes were drilled in summer 2000 in the Murtèl-Corvatsch rock glacier, which is located in the Upper Engadin, Swiss Alps (e.g. Haeberli et al. 1998). Several cores were drilled, transported and stored at about -18°C and then tested in the laboratory in a triaxial apparatus in a cold room at temperatures between -1 and -5°C (Arenson 2002).

Seven pressuremeter tests were carried out in borehole 1/2000 at various depths after the borehole had been drilled below the planned test (Table 1).

Table 1. Overview of all pressuremeter tests.

Test No.	Depth ¹	Pocket diam	Tests ²	Soil characteristics
	[m]	[mm]		Ice / Solids / Air ³
				[vol.-%]
1	14.7 (23)	107.2	s	ice (with some sand ⁴) 90 / 0 / 10
2	16.0 (23)	105.1	3 cr 2 ul	ice (with some sand ⁴) 90 / 0 / 10
3	18.5 (27)	98.8	5 cr 3 ul	ice with some gravel and sand 80 / 4 / 16
4	21.2 (23)	104.2	4 cr 3 ul	ice with some silt and sand 80 / 4 / 16
5	22.5 (27)	101.0	4 cr 3 ul	ice with gravel and sand 77 / 8 / 15
6	23.4 (27)	104.7	s	ice with coarse gravel and sand: 80 / 8 / 12
7	24.5 (27)	113.3	5 cr 4 ul 2 r	ice with coarse gravel and sand: 86 / 8 / 6

¹ Depths in brackets denote depth of borehole at time of test

² s: shear test; cr: creep stages; ul: unload-reload loops; r: relaxation

³ From sample analyses

⁴ Less than 0.3%

The composition of the soil at these depths was determined in the laboratory, after the sample had been tested under triaxial conditions.

The creep of frozen material is strongly dependent on the temperature. Thermal disturbances in the soil close to the borehole have to be expected due to the drilling process, even though this was carried out with cold-air-flushing at the drill bit. Furthermore, the time between drilling to the required depth and the start of the pressuremeter test was not long enough for the ground temperature to level off at its previous thermal condition. Temperature measurements within the pressuremeter probe showed that the probe was also not at the exact soil temperature initially. However, as can be shown from the test data, these temperature differences between the probe, the borehole wall and the remaining soil only appear to have influenced the results for the first holding stage(s). At this stage, an expeditious balance between preventing excessive relaxation (and perhaps spalling) in the borehole wall, an appropriate temperature regime in the ground and timely completion of the project played a part in taking these decisions.

Approximate borehole temperatures at the selected depths were available from continuous temperature measurements in the nearby borehole 2/1987, (Vonder Mühl et al. 1998). The chosen depths are at or just below the zero annual amplitude of this particular rock glacier, i.e. the temperatures remain constant throughout the year. The temperature increases from -1.8°C at a depth of 14.7 m to -1.5°C at 24.5 m.

3 THEORY OF BOREHOLE CREEP TESTS

3.1 Pressuremeter creep

Methods of determining creep parameters from borehole creep tests have been presented by various authors (Ladanyi & Johnston 1973, Kjartanson et al. 1988, Ladanyi & Melouki 1992). Since the test duration for a multi-stage creep test is usually short, Ladanyi & Johnston (1973) recommend considering the test as being essentially of a primary creep type, that can be solved for the creep strain $\epsilon_{e,c}$ as a function of time t , with Andrade's empirical law, recommended by Hult (1966) and Ladanyi (1972):

$$\epsilon_{e,c} = \left(\frac{\dot{\epsilon}_c}{b} \right)^b \left(\frac{q}{\sigma_c} \right)^{n_1} t^b \quad (1)$$

where a creep factor A can be defined as:

$$A = \left(\frac{\dot{\epsilon}_c}{b} \right)^b \sigma_c^{-n_1} \quad (2)$$

and where b , n_1 are additional creep parameters to be determined from *in situ* tests, $\dot{\epsilon}_c$ is a reference strain

rate related to a reference creep stress σ_c and q the applied creep stress.

A different approach using *Glen's flow law* (Glen 1955) was proposed by (Kjartanson et al. 1988), assuming that steady-state (secondary) creep is reached:

$$\left(\frac{\dot{r}}{r}\right)_{\min} = ap^{n_2} \quad (3)$$

where a , n_2 are the creep parameters, p is the pressure within the pressuremeter and $(\dot{r}/r)_{\min}$ is the minimum value of the radial strain rate and is equal to $\dot{\epsilon}_{c,\min}$.

For both cases, the stress redistribution before and during each additional loading step (after Murat et al. 1989) has to be considered, which takes the time dependent reduction of the stress in the ground into account.

3.2 Triaxial creep versus pressuremeter creep

If the results of the pressuremeter creep tests are to be compared with those obtained from triaxial creep tests, the stress states as well as the degrees of freedom of deformation must be considered. In a pressuremeter test, a length of the borehole is expanded by a radially acting pressure, whereas a cylindrical sample is subjected to a hydrostatic cell pressure and then held constant under compression in a triaxial creep test (Fig. 1). The stresses therefore do not remain constant in all directions. Assuming elasticity, which is valid for analysing the early stages of the pressuremeter test, the circumferential stress σ_θ is reduced by the same increment Δp as the radial stress $\sigma_r = p$ increases. The vertical stress σ_z is assumed to remain constant. Under triaxial stress conditions, only the axial stress σ_1 increases, while the radial stress σ_3 is held constant during the test. Therefore the first stress invariant was used for comparison:

$$q = \frac{1}{\sqrt{2}} \sqrt{(\sigma_1 - \sigma_2)^2 + (\sigma_2 - \sigma_3)^2 + (\sigma_3 - \sigma_1)^2} \quad (4)$$

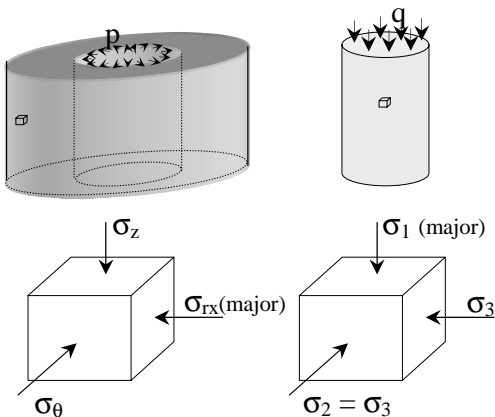


Figure 1. Principal stress systems acting on an element in a pressuremeter test (left) and a triaxial test (right).

The principal stresses are different in the three orthogonal directions for a pressuremeter test, and are assumed to be: vertical stress σ_z , radial stress σ_r and the circumferential stress σ_θ . Assuming isotropic elastic conditions (earth pressure coefficient at rest $K_0 \approx 1$) all *in situ* stresses are equal at the beginning $\sigma_{z(t=0)} = \sigma_{r(t=0)} = \sigma_{\theta(t=0)}$. During the test, the pressure within the pressuremeter probe (p) increases and with $\Delta p = p - \sigma_{r(t=0)}$, the stresses at time t are:

$$\sigma_z = \sigma_{z(t=0)}, \text{ constant throughout the test} \quad (5)$$

$$\sigma_r = \sigma_{r(t=0)} + \Delta p = \sigma_z + \Delta p \quad (6)$$

$$\sigma_\theta = \sigma_{r(t=0)} - \Delta p = \sigma_z - \Delta p \quad (7)$$

Substituting Equations 5 – 7 into Equation 4, the first stress invariant, in the case of a pressuremeter test, is:

$$q = \sqrt{3} \cdot \Delta p \quad (8)$$

In the case of a triaxial creep test, that is started after an isotropic consolidation with $\sigma_1 = \sigma_2 = \sigma_3$, the first stress invariant is equal to the deviatoric stress q :

$$q = \sigma_1 - \sigma_3. \quad (9)$$

4 RESULTS OF PRESSUREMETER TESTS

4.1 Creep tests

Typical creep curves are shown in Figure 2 for tests carried out at 18.5 m and 24.5 m depth, respectively. The cavity pressures for the test at 24.5 m have been higher than for the other test and therefore, larger creep strain rates occurred, resulting in steeper curves and in a shorter test duration.

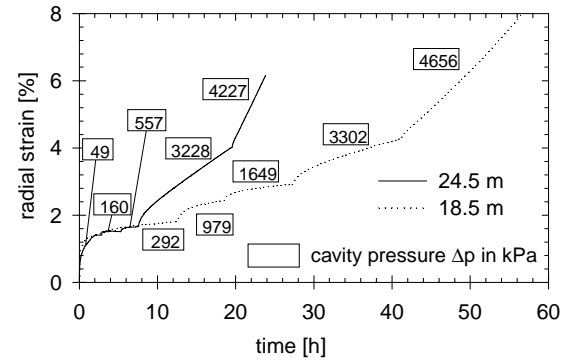


Figure 2. Multi-stage pressuremeter tests within borehole 1/2000, Murtèl-Corvatsch rock glacier.

For the first creep stages, i.e. low pressures within the pressuremeter, the radial creep strain rates $\dot{\epsilon}_c$ have a large scatter due temperature and drilling disturbances. With increasing pressure, however, the variation in $\dot{\epsilon}_c$ decreases (Fig. 3).

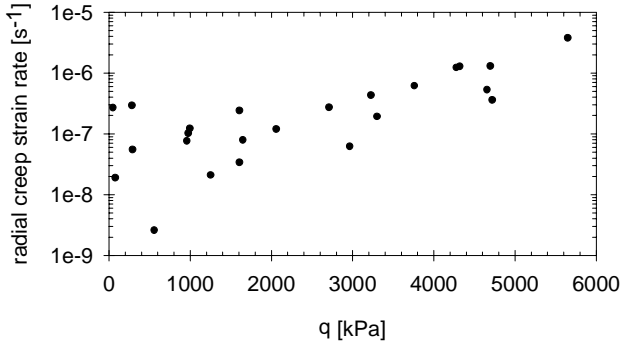


Figure 3. Radial creep strain rates for all tests.

Using the primary creep approach, expressed by Equation 1, the following creep parameters n_1 , b and A can be found (Table 2):

Table 2. Creep parameters after Equation 1: $\epsilon_{e,c} = Aq^{n_1}t^b$

Test	n_1	b	A [min ^{-b}]	ice	soil	air
2	1.04	0.66	$2.0 \cdot 10^{-8}$	90	0	10
3	1.16	0.61	$2.3 \cdot 10^{-8}$	80	4	16
4	1.00	0.69	$5.6 \cdot 10^{-8}$	80	4	16
5	1.40	0.82	$2.8 \cdot 10^{-9}$	77	8	15
7	1.86	0.75	$1.3 \cdot 10^{-10}$	86	8	6

Analysing the five tests where creep stages were applied with Equation 3, creep parameters can be determined as shown in Table 3, where the accuracy of the creep function with the effective values is denoted by a correlation coefficient R^2 .

Table 3. Creep parameters after Equation 3: $\dot{\epsilon}_c = aq^{n_2}$

Test	a	n_2	R^2
2	$7.0 \cdot 10^{-15}$	2.08	0.91
3	$7.3 \cdot 10^{-10}$	0.73	0.76
4	$2.7 \cdot 10^{-10}$	0.90	0.82
5	$4.0 \cdot 10^{-12}$	1.57	0.69
7	$1.4 \cdot 10^{-17}$	3.29	0.98

4.2 Failure tests

At the end of all five multi-stage creep tests, the radial pressure was increased constantly with a radial strain rate of about $7 \cdot 10^{-6} \text{ s}^{-1}$. Test No 1 (14.7 m) has to be ignored, since the temperature in the probe was above zero centigrade and therefore the probe melted its way through the ice. Consequently, much higher radial strain was recorded for a similar cavity pressure. For most of tests, a cavity pressure of just above 3 MPa was applied before the test had to be stopped due to uneven recordings of the six displacement transducers. Such response is possible, when the probe moves within the borehole, indicating that the soil properties are not homogeneous around the borehole. However, for the depths tested, a yield stress between 2 and 3 MPa can be determined (Fig. 4) at a radial strain of about 2.7 – 2.8%.

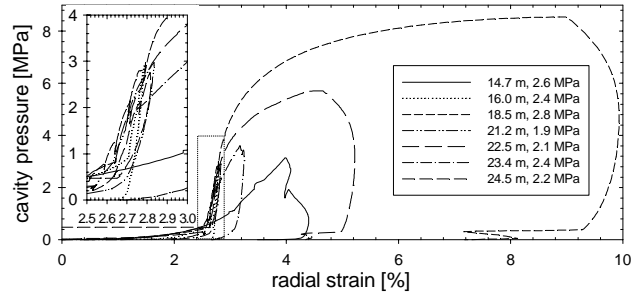


Figure 4. Shearing phase: maximum cavity pressure and lower yield stress.

Unload-reload loops were performed between the creep stages with a reduction of radial strain $\Delta\epsilon_r$ up to 0.04%. Shear moduli G could be calculated using Equation 10.

$$G = \frac{1}{2} \frac{\Delta\sigma_r}{\Delta\epsilon_r} \quad (10)$$

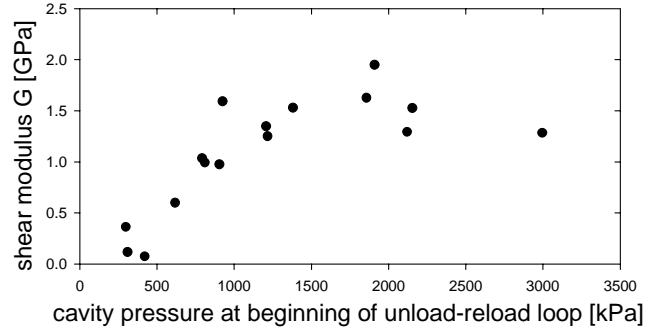


Figure 5. Shear moduli as a function of mean cavity pressure during the unload reload loop.

Even though the material seems to creep unequally, the moduli are quite consistent at each unloading stage over the chosen depths. Rather than varying as a function of the depth, the shear modulus depends on the applied cavity pressure. However, this influence wears off with increasing mean pressure in the borehole.

5 TRIAXIAL TEST RESULT

The most appropriate triaxial test for comparison with pressuremeter data was performed on a sample from a depth of between 22.72 – 22.87 m and was carried out at a temperature of -1.15°C , with a confining pressure of 200 kPa. For this sample, which had a volumetric ice content of 77% and 8% solids, the following creep relationship could be determined with an accuracy $R^2 = 0.98$ (after Glen's flow law):

$$\dot{\epsilon}_{axial} = a \cdot q^n \quad (11)$$

$$a = 2 \cdot 10^{-13} \text{ s}^{-1} \text{ kPa}^{-2.42}, n = 2.42$$

Additional tests that were carried out at a temperature of -4.1°C showed lower a values (this is the temperature dependent parameter) and n_2 values that increased with depth, from 2.3 to 3.7 at 13.9 and 25.0 m, respectively.

6 DISCUSSION AND CONCLUSIONS

In situ testing, e.g. using a pressuremeter is highly recommended to determine *in situ* soil conditions and properties, since the disturbance of the ground can be kept to a minimum. However, in the case of rock glacier material, where the range of particle sizes and the air voids can be extremely high, the soil parameters may vary considerably within a few metres, and even *in situ* testing can be very unsatisfactory. The results might not be representative of the macro response of the rock glacier and they can be strongly influenced by thermal and mechanical disturbances of the soil as well. Numerous tests are therefore necessary. Nevertheless it is possible to detect trends and to evaluate a range of soil parameters.

Two different methods had been used for the analyses of the *in situ* creep parameters based either on a primary creep or a steady state (secondary creep) approach. Both methods indicate similar trends. However, the parameters are very sensitive to small changes during the test and therefore have to be analysed critically. Since the first method uses the strain at a reference time shortly after the test has started, the strain might still be influenced by the bedding in of the probe and local re-distribution of small strains or air voids. On the other hand, it is difficult to obtain steady state or minimum creep within a day. The strain rates often had to be extrapolated in order to obtain a constant value.

The dependency of the creep parameters on depth is shown in Figure 6. Both stress exponents n_1 and n_2 increase with depth and the multipliers A and a , respectively, tend to decrease. However, in the first case, the test at a depth of 21.2 m and in the second case, at 16.0 m have to be analysed carefully. A jump in the secondary creep response at 24 m can be observed, where n_2 increases rapidly as a decreases. This can be explained by a higher percentage of solid particles and a lower content of air voids.

In contrast to test No. 5 (22.5 m), the volumetric air content is much lower for test No. 7 (24.5 m) and therefore, volumetric change and hence radial strain rate will be lower. The soil at greater depths therefore tends to be less creep susceptible. This observation fits well with the measured deformation profile in borehole 1/1987 (e.g. Arenson et al. 2002) and estimated shear surface determined by georadar (Lehmann & Green 2000) indicating a shear horizon at a depth of about 25 m at the location of this borehole.

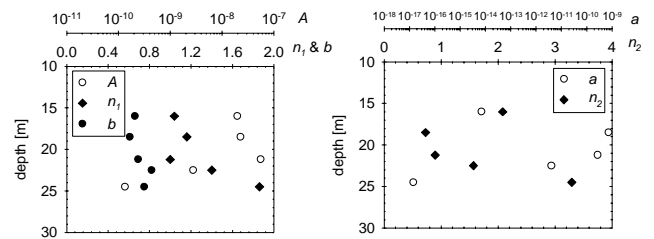


Figure 6. Creep parameters: primary creep approach (left), secondary creep approach (right).

An analysis of these pressuremeter tests is possible using a primary creep as well as a secondary creep approach. Due to the relatively short time the soil is maintained under a constant pressure, it is reasonable to use a primary creep approach that includes the change in the strain rate with time. The model presented by Ladanyi and Johnston (1973) has been used to reconstruct strains developing during a creep test (Fig. 7). This has been very effective for the three middle stages.

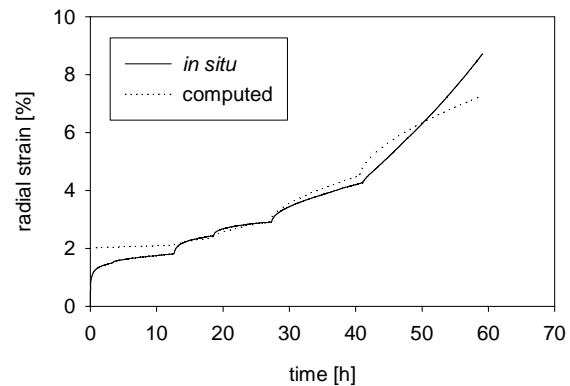


Figure 7. Multi-stage pressuremeter creep test at a depth of 18.5 m. Original and computed data.

However, some aspects have to be considered when computing data from *in situ* tests using a primary creep approach.

- Large strains at the beginning of a test, due to effects described in chapter 2, cannot be modelled and therefore differences in total strain occur.
- The model assumes an ongoing decrease in the radial creep rate. Therefore, it is not possible to determine secondary creep parameters.
- Tertiary creep will be ignored.

By adopting a moving average and extrapolating the data of strain rates against time towards an asymptote, a minimum creep strain rate may be estimated. Analysing these minimum creep strain rates versus the first stress invariant for pressuremeter tests, reasonable results were obtained, that are also comparable with data from triaxial creep tests (Fig. 8).

Pressuremeter tests have been used as an alternative method of determining *in situ* creep properties for Alpine permafrost. However, due to the extreme heterogeneity of Alpine soil conditions, it is essen-

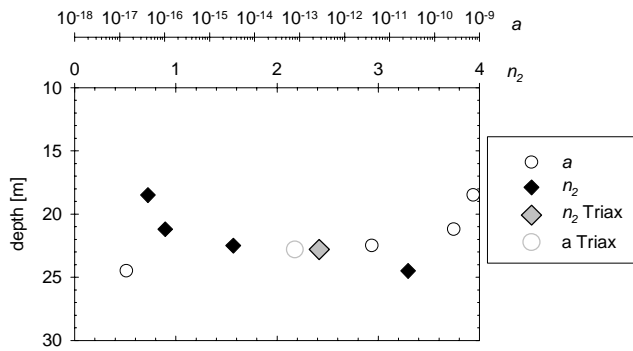


Figure 8. Secondary creep parameters for pressuremeter and triaxial creep tests.

tial to perform a number of tests at various depths and locations. In addition, exceptional care has to be taken while drilling and preparing the testing probe. Both aspects are responsible for the test quality. While careful drilling results in better borehole stability and a smoother borehole wall, temperature equalisation of the probe minimises thermal disturbances. Furthermore, pressuremeter tests might even be possible in conditions where sampling is nearly impossible. This is certainly a cost-effective test and should be considered for future investigations.

ACKNOWLEDGEMENT

The authors wish to thank the Swiss Federal Institute of Technology Research Commission for their financial support. In addition we gratefully acknowledge everybody who helped during the field campaign, Stump Bohr AG for drilling the boreholes, the Oberengadiner Bergbahnen for their support during all the fieldwork and Heli-Bernina for flying the team and the equipment onto the rock glacier.

REFERENCES

Arenson, L.U. 2002. Unstable Alpine permafrost: a potentially important natural hazard – Variations of geotechnical behaviour with time and temperature. *PhD No 14801, Inst. for Geotech. Engng., ETH, Zurich*.

Arenson, L.U. & Springman, S.M. 2000. Slope stability and related problems of Alpine permafrost. *Proc. Int. Workshop Permafrost Eng., Longyearbyen*: 185-196.

Arenson, L.U., Almasi, N. & Springman, S.M. 2003. Shearing response of ice-rich rock glacier material. *Proc. 8th Int. Conf. on Permafrost, Zurich*: this issue.

Arenson, L.U., Hoelzle, M. & Springman, S.M. 2002. Borehole deformation measurements and internal structure of some rock glaciers in Switzerland. *Permafrost and Periglacial Processes* 13(2): 117-135.

Cheng, G. & Dramis, F. 1992. Distribution of mountain permafrost and climate. *Permafrost and Periglacial Processes* 3(2): 83-91.

Fragaszy, R.J., Su, W. & Siddiqi, F.H. 1990. Effects of oversize particles on the density of clean granular soils. *ASTM Geotechnical Testing Journal* 13: 106-114.

Glen, J.W. 1955. The creep of polycrystalline ice. *Proc. Roy. Soc. London A*228: 519-538.

Haerberli, W., Cheng, G., Gorbunov, A.P. & Harris, S.A. 1993. Mountain permafrost and climate change. *Permafrost and Periglacial Processes* 4(2): 165-174.

Haerberli, W., Wegmann, M. & Vonder Muehll, D. 1997. Slope stability problems related to glacier shrinkage and permafrost degradation in the Alps. *Eclogae Geologicae Helveticae* 90: 407-414.

Haerberli, W., Hoelzle, M., Käab, A., Keller, F., Vonder Muehll, D. & Wagner, S. 1998. Ten years after drilling through the permafrost of the active rock glacier Murtèl, eastern Swiss Alps: Answered questions and new perspectives. *Proc. 7th Int. Conf. on Permafrost, Yellowknife*: 403-410.

Hauck, C., Guglielmin, M., Isaksen, K. & Vonder Muehll, D. 2001. Applicability of frequency-domain and time-domain electromagnetic methods for mountain permafrost studies. *Permafrost and Periglacial Processes* 12(1): 39-52.

Harris, C. Haerberli, W., Vonder Muehll, D. & King, L. 2001. Permafrost monitoring in the high mountains of Europe: the PACE project in its global context. *Permafrost and Periglacial Processes* 12(1): 3-11.

Hult, J.A.H. 1966. *Creep in engineering structures*. Waltham, Massachusetts: Blaisdell Publ. Co.

Käab, A. & Vollmer, M. 2000. Surface geometry, thickness changes and flow fields on creeping mountain permafrost: Automatic extraction by digital image analysis. *Permafrost and Periglacial Processes* 11(4): 315-326.

Kjartanson, B.H., Shields, D.H., Domaschuk, L. & Man C.S. 1988. The creep of ice measured with the pressuremeter. *Canadian Geotechnical Journal* 25: 250-261.

Ladanyi, B. 1972. An engineering theory of creep of frozen soils. *Canadian Geotechnical Journal* 9: 63-80.

Ladanyi, B. 1982. Borehole creep and relaxation tests in ice-rich permafrost. *Proc. 4th Can. Permafrost Conf., Calgary*: 406-415.

Ladanyi, B. & Huneault, P. 1987. Use of borehole relaxation test for determining the creep properties of ice. *Proc. 6th Int. Offshore Mech. and Arct. Eng. Symp., Houston*: 253-259.

Ladanyi, B. & Johnston, G.H. 1973. Evaluation of in situ creep properties of frozen soils with the pressuremeter. *Proc. 2nd Int. Conf. on Permafrost, Yakutsk*: 310-318.

Ladanyi, B. & Melouki, M. 1992. Determination of creep properties of frozen soils by means of borehole stress relaxation test. *Canadian Geotechnical Journal* 30: 170-186.

Lehmann, F. & Green, A. 2000. Topographic migration of georadar data: Implications for acquisition and processing. *Geophysics* 64: 836-848.

Murat, J.R., Ladanyi, B. & Huneault, P. 1989. In situ determination of creep properties of sea ice with the pressuremeter. *Canadian Geotechnical Journal* 26: 575-594.

Musil, M., Maurer, H., Green, A.G., Horstmeyer, H., Nitsche, F.O., Vonder Muehll, D. & Springman S. 2002. Shallow seismic surveying of an Alpine rock glacier. *Geophysics* 67: 1701-1710.

Vonder Muehll, D., Stucki, T. & Haerberli W. 1998. Borehole temperatures in Alpine permafrost: a ten year series. *Proc. 7th Int. Conf. on Permafrost, Yellowknife*: 1089-1095.

Wagner S. 1992. Creep of Alpine permafrost, investigated on Murtèl rock glacier. *Permafrost and Periglacial Processes* 3: 157-162.

Williams, P.J. 1967. Unfrozen water content of frozen soils and soil moisture suction. *Publication of the Norwegian Geotechnical Institute* 72: 11-26.